Supporting Information

MoC nanodots toward efficient electrocatalytic hydrogen evolution: An interlayer-confined strategy with 2D-zeolite precursor

Boxu Gao[a], Yanghuan Huang[a], Sinong Wang[b*], Haiyang Lu[a], Luyao Zheng[a], Xueliang Fan[a], Xue Yang[a], Wenbiao Zhang[c], Yajun Wang[d], Yahong Zhang[a], Qingsheng Gao[c*] and Yi Tang[a*]

a. Department of Chemistry, Shanghai Key Laboratory of Molecular Catalysis and Innovative Materials, Laboratory of Advanced Materials and Collaborative Innovation Center of Chemistry for Energy Materials, Fudan University, Shanghai 200433, China. E-email: yitang@fudan.edu.cn

b. Institute for Preservation of Chinese Ancient Books, Fudan University Library, Fudan University, Shanghai 200433, China. E-email: wangsn@fudan.edu.cn

c. Department of Chemistry, Jinan University, Guangzhou 510632, China. E-email: tqsgao@jnu.edu.cn

d. College of Chemistry & Materials Engineering, Wenzhou University, Zhejiang 325027, China

Synthesis of MCM-22 precursor

A hydrothermal method is used for synthesizing MCM-22 precursor. A sol is obtained by mixing NaOH, $NaAlO_2$, HMI and silica sol together with water under vigorously stirring at a specific mole ratio (SiO_2 : Al_2O_3 : Na_2O : HMI : H_2O = 1 : 0.2 : 0.1 : 0.5 : 18). The sol is aged for 1 h at room temperature and transferred into a Teflon lined stainless-steel autoclaves and heated at 150 °C, rotated at 20 rpm for 3 days. The sample is filtered and washed with deionized water adequately. The solid product is dried at 80 °C overnight to achieve MCM-22 precursor.

Synthesis of reference samples

The sample obtained without MCM-22(P) (named MoC_x-wm) is synthesized through directly pyrolyzing the complex of AHM and CTAB (named Mo-CTAB), which is achieved by the hybrid of 0.25 g CTAB and 0.625 g AHM under the same condition with Mo-MCM-x, at 750°C for 5 h. The physical mixture sample (named MoC_x-pm-0.5) is obtained by pyrolyzing the powder mixture of MCM-22(P) and Mo-CTAB product at 750°C for 5 h with a same feed ratio with Mo-MCM-0.5.

Structure characterization

Powder X-ray diffraction (XRD) patterns of all the samples are recorded from a Bruker D2 Advance diffractometer with Cu Kα radiation at 30 kV and 10 mA. Fourier transform infrared (FTIR) spectra of the precursors are recorded by a ThermoFisher Nicolet iS10 FTIR spectrometer. The structures, morphologies and related element mapping images are obtained by scanning electron microscopy (SEM, Hitachi S-4800) and transmission electron microscopy (TEM, FEI Tecnai G2 F20 S-Twin). Thermogravimetric analysis (TGA) is obtained on a thermal analyzer (SDT Q600) with a heating rate of 10 °C·min^{-1} under air flow. Raman spectrum is collected on the laser confocal Raman microspectrometer (XploRA, Horiba Jobin Yvon, Ltd.) with an excitation wavelength of 532 nm. X-ray photoelectron spectroscopy (XPS) is collected by scanning Xray microprobe (Thermo Scientific, ESCALAB 250Xi) using Al Kα radiation and the C 1s peak at 284.6 eV as the internal standard.

Electrochemical measurements

The working electrode is a glassy carbon electrode (GCE, 3.0 mm in diameter) modified

by the following steps before test. (1) 10 mg of as-prepared catalyst is dispersed in a mixed solution containing 750 μL of water, 250 μL of ethanol and 40 μL of 5 wt. % Nafion solution by ultrasonication for 1 h to form a homogeneous suspension. (2) 8 μL of the ink is loaded onto the surface of the GCE. (3) The GCE is dried at room temperature. The potential is converted to the potential versus reversible hydrogen electrode (RHE) according to E(RHE) = E(SCE) + 0.2412 + 0.059pH. Before the test, the working electrode was activated at least 30 times at a scan rate of 50 $mV \cdot s^{-1}$. Linear sweep voltammetry (LSV) is recorded at a scan rate of 5 $mV \cdot s^{-1}$ with iR-correction in 0.5 M H_2SO_4 (pH 0.3), 1 M phosphate buffer (PB, pH 7) and 1 M KOH (pH 14). Long term stability test is performed by repetitive LSV at a scan rate of 50 $mV \cdot s^{-1}$. Chronoamperometry (CA) is also tested under η = 150 mV (versus RHE) without iR-correction for 10 hours. Cyclic voltammograms (CV) is obtained from 0 to 0.3 V (versus RHE) under different sweep rates of 10, 25, 50, 75, 100, 150, 200, 250 and 300 $mV \cdot s^{-1}$. Electrochemical impedance spectroscopy (EIS) is performed with the frequency range from 0.01 to 106 Hz with an AC voltage of 5 mV.

The calculation of turnover frequency (TOF) value

The TOF values of our catalysts are calculated in all conditions. We assume that the Faraday efficiency is 100% and all the Mo atoms on the electrode are active sites [S1]. The calculation of the TOF value follows the functions below:

$$TOF = n(H_2) / n(Mo)$$

$$n(H_2) = (j_{\eta = 150} * S * N_A) / (n * F)$$

$$n(Mo) = m_{sample\ loading} * c\ wt.\ \% * N_A / M(MoC)$$

Here n (H_2) represents the number of theoretic Hydrogen molecules produced per second, which is obtained at an overpotential of 150 mV ($j_{\eta = 150}$) for all the conditions; S represents the surface area of glassy carbon electrode; N_A is the Avogadro's number (6.02×10^{23} mol^{-1}); n is the electro transfer number (2 for Hydrogen) per molecule; F is the Faraday constant (96485 C mol^{-1}); n (Mo) represents the number of active Mo atoms on the electrode; *c* wt. % is the content of MoC in the initial sample.

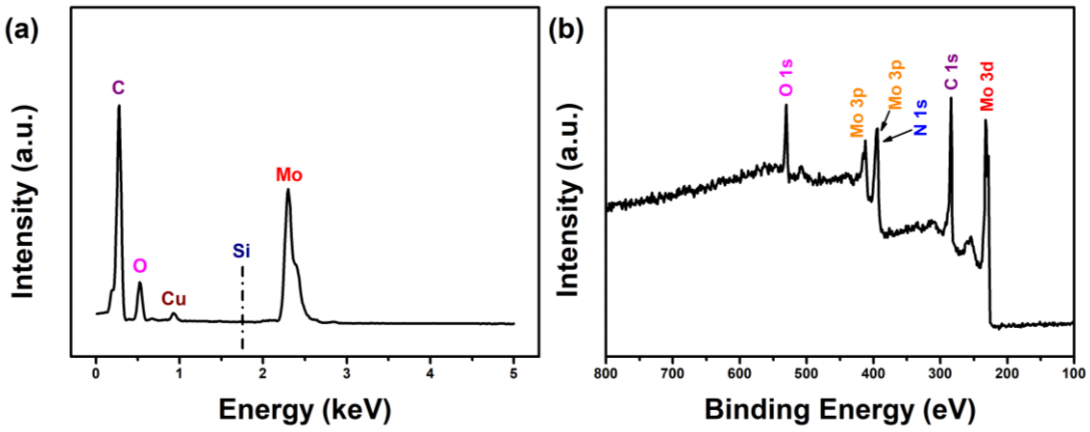

Fig. S1. EDS result (a) and XPS spectrum (b) of nano-MoC/C-Ns-0.5 sample. The Kα characteristic X-ray energy for Si element marked on the graph (a) is applied to show the complete removal of zeolite after HF etching.

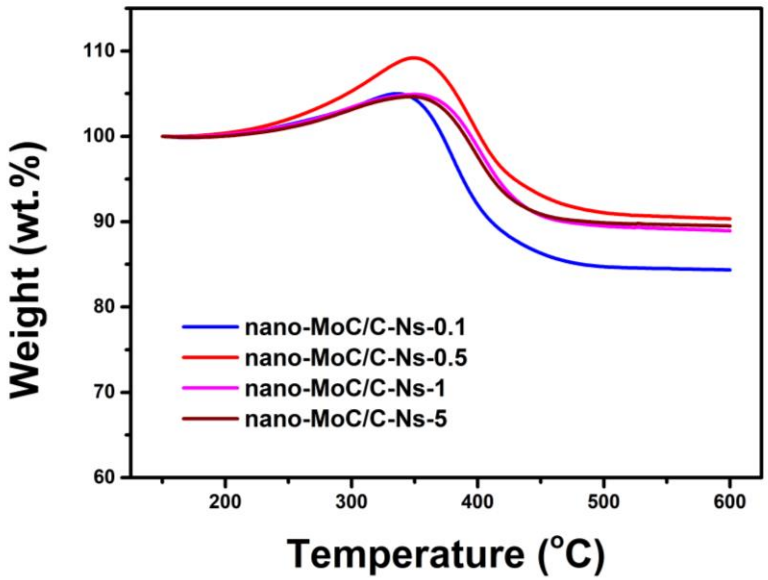

Fig. S2. TGA curves for nano-MoC/C-Ns-x samples. We assume that MoC samples only consist of MoC and free carbon and convert to MoO_3 after 600°C. The total weight loss is *a* %. The content of MoC in the initial sample (*c* wt. %) is calculated by the following equation: *c* wt. % = *a* % * M (MoC) / M (MoO_3). The weight loss before 150 °C is omitted because the weight loss in this period is attributed to the physically adsorbed water and the weight at 150 °C is considered as the initial sample weight.

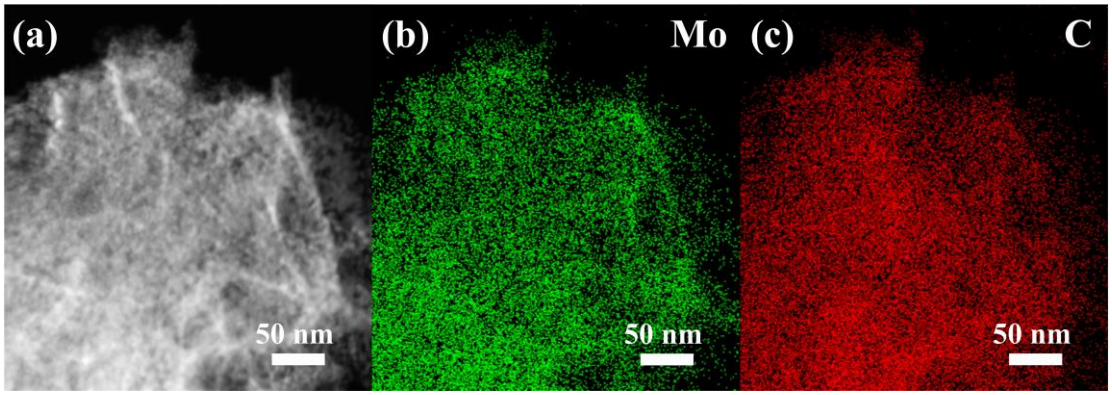

Fig. S3. STEM image (a) and corresponding elemental mappings (b, c) for nano-MoC/C-Ns-0.5 sample.

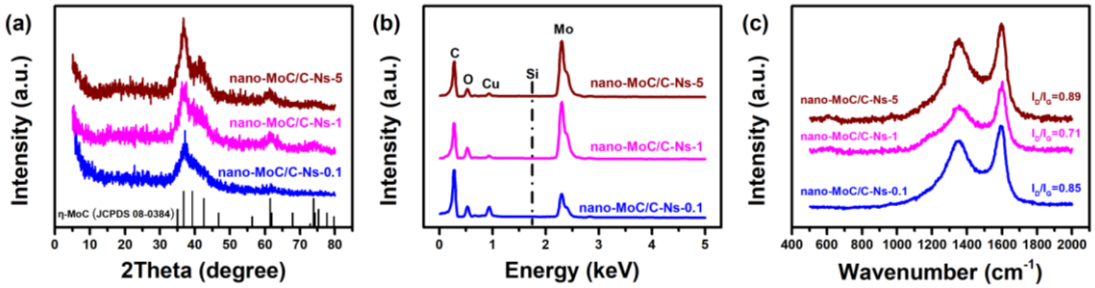

Fig. S4. XRD patterns (a), EDS results (b), and Raman spectra (c) of nano-MoC_x/C-Ns-0.1, nano-MoC_x/C-Ns-1 and nano-MoC_x/C-Ns-5 samples. The Kα characteristic X-ray energy for Si element marked on the graph (b) is applied to show the removal of zeolite after HF etching.

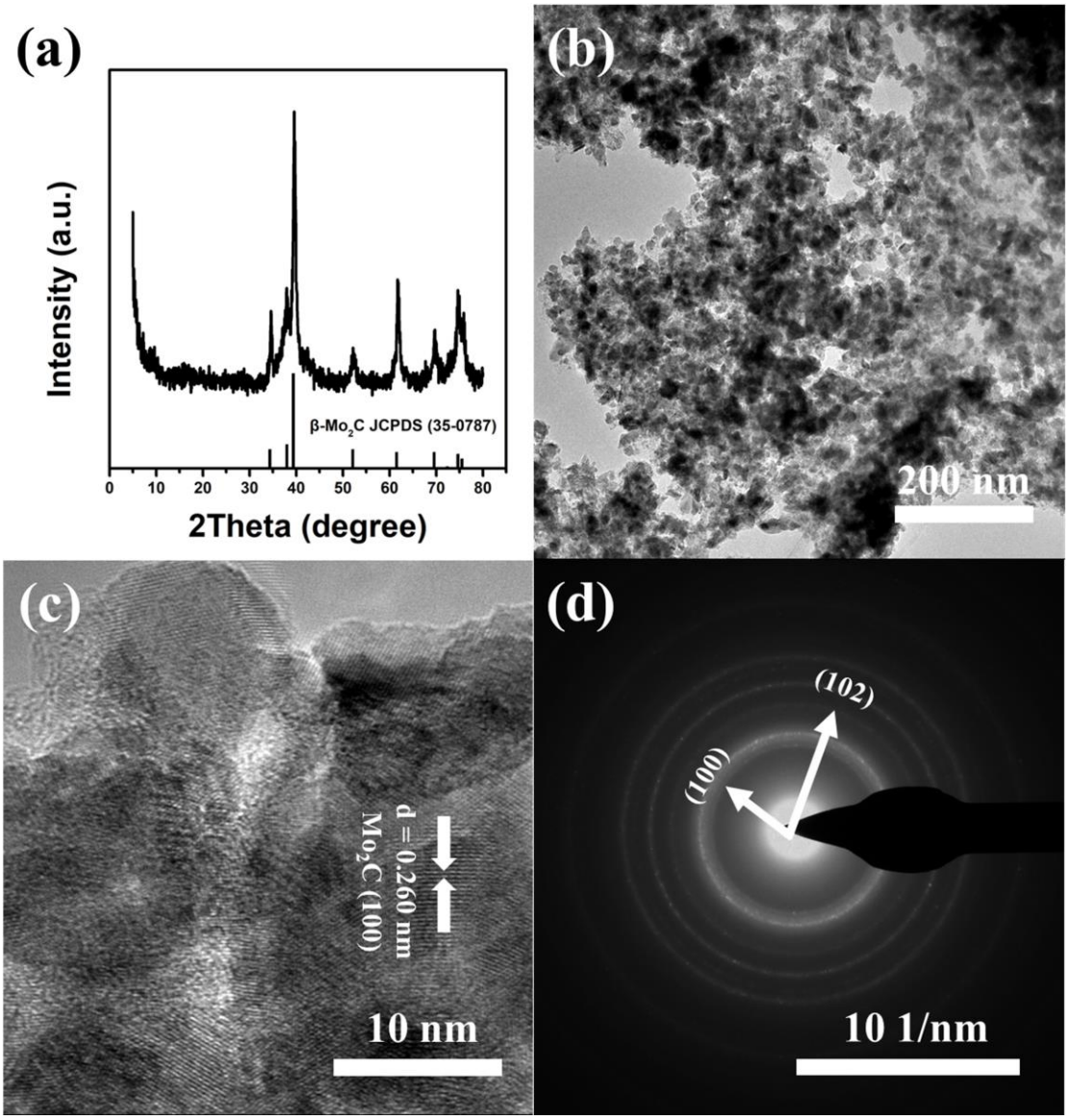

Fig. S5. (a) XRD pattern, (b) TEM image, (c) HRTEM image and (d) SEAD pattern for MoC_x-wm.

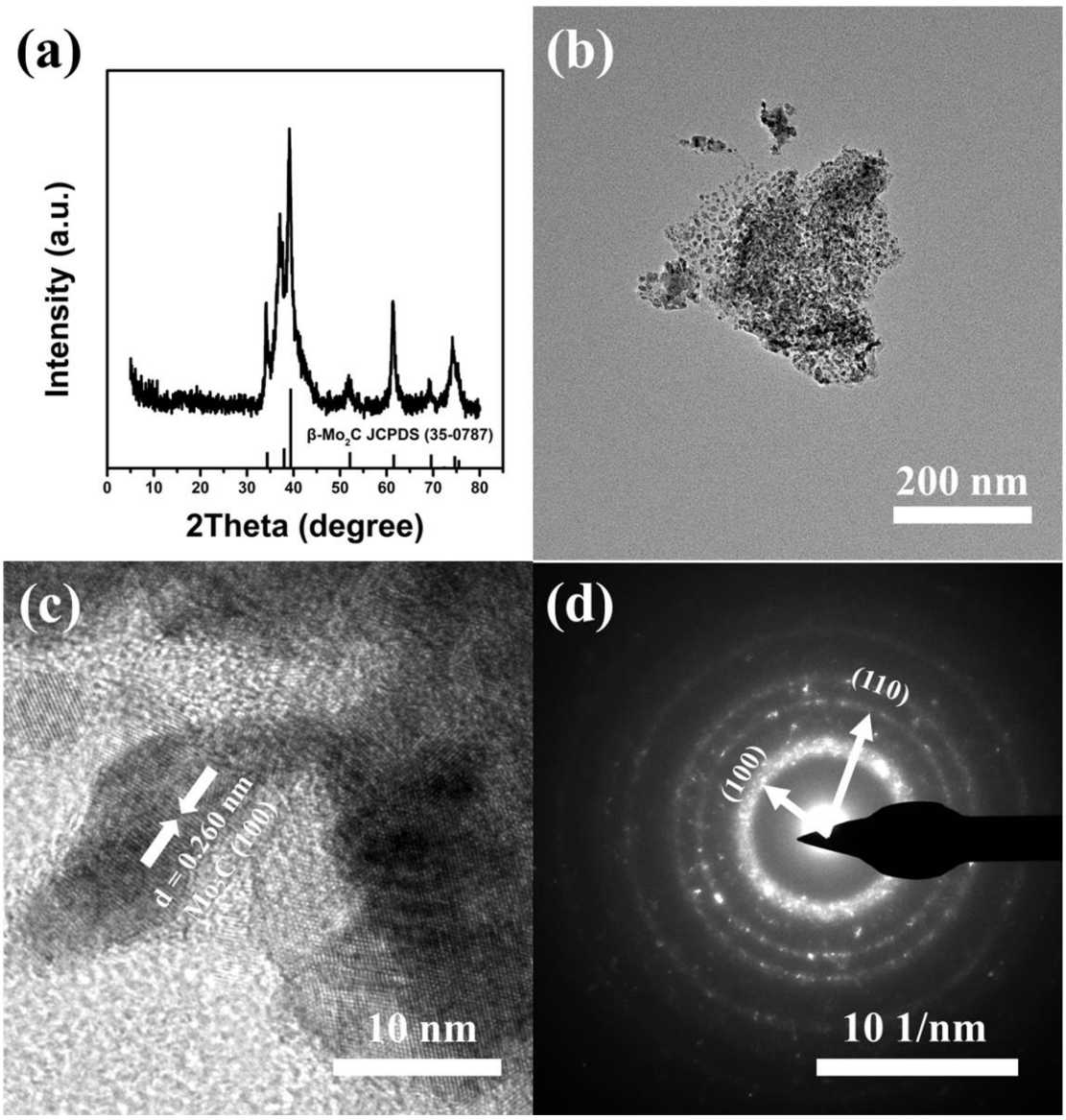

Fig. S6. (a) XRD pattern, (b) TEM image, (c) HRTEM image and (d) SEAD pattern for MoC_x-pm-0.5.

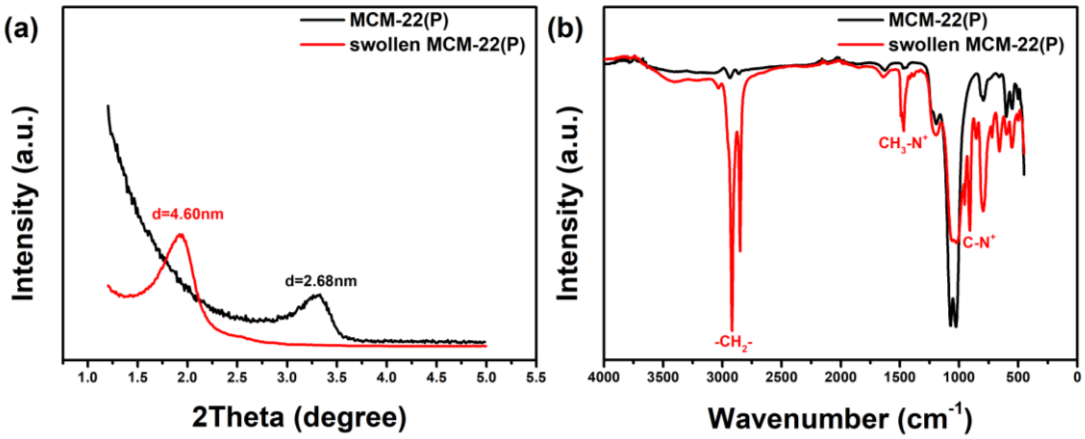

Fig. S7. Small angle XRD patterns (a) and FTIR spectra (b) for MCM-22(P) and swollen MCM-22(P).

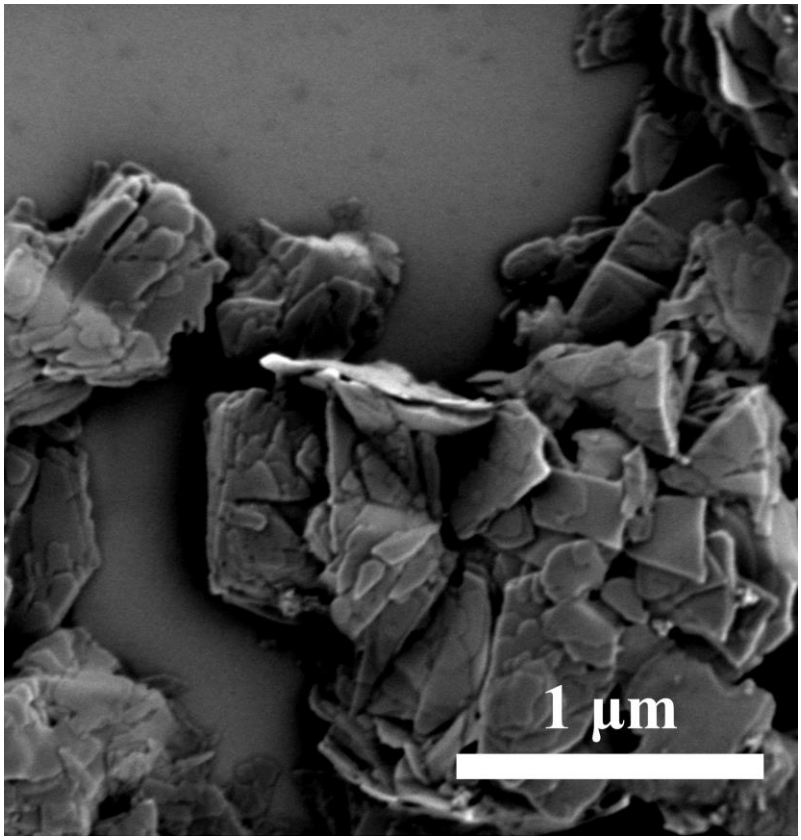

Fig. S8. SEM image for swollen MCM-22(P).

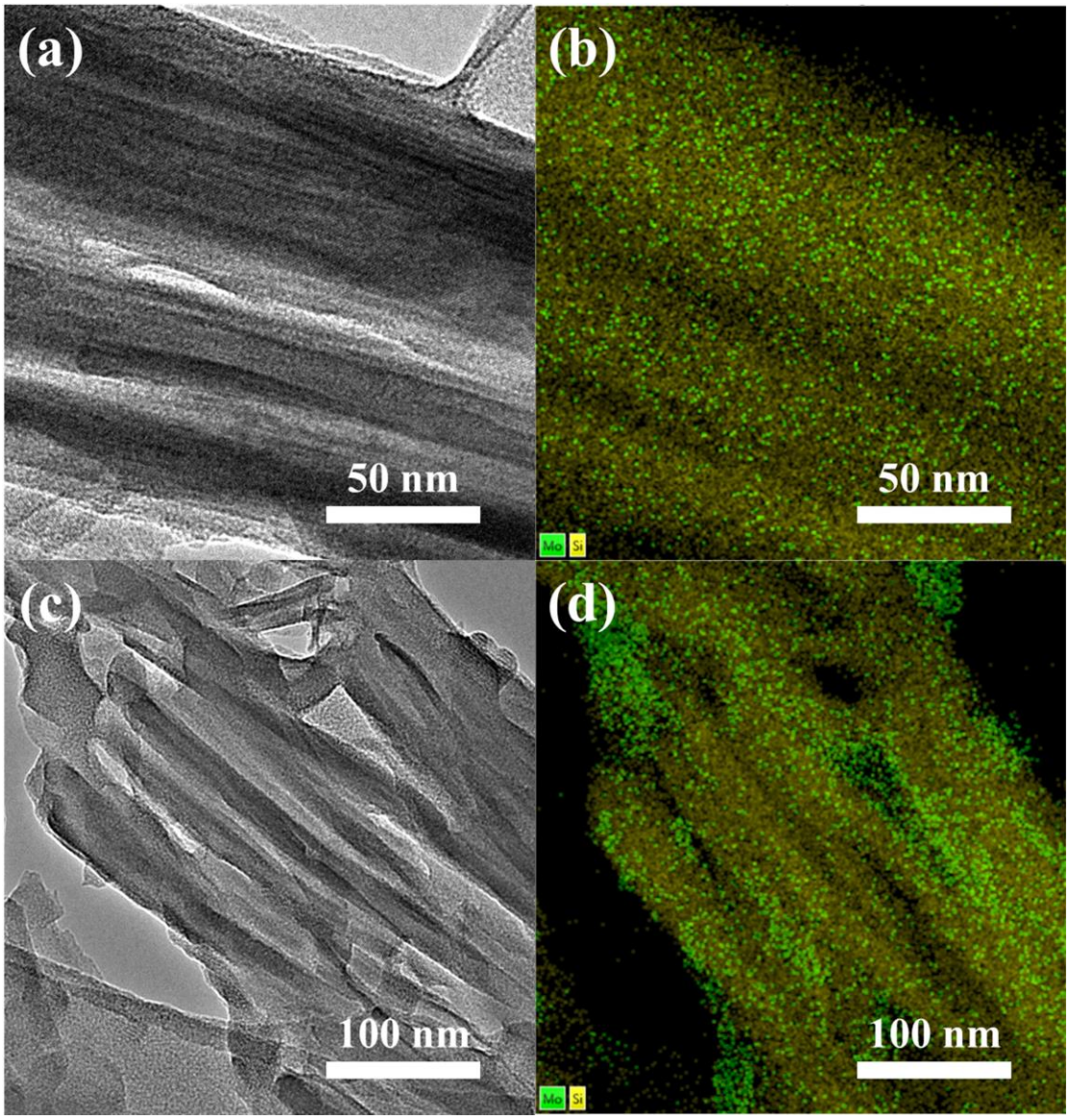

Fig. S9. TEM image and corresponding elemental mapping for Mo-MCM-0.5 (a-b) and Mo-MCM-5 (c-d) sections.

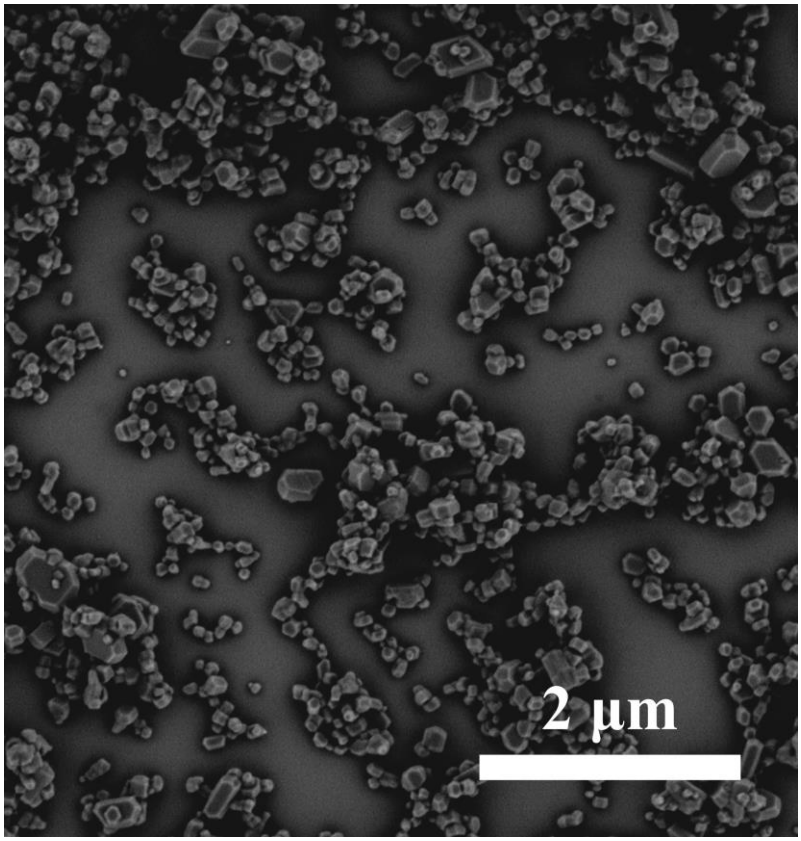

Fig. S10. SEM image for Mo-CTAB.

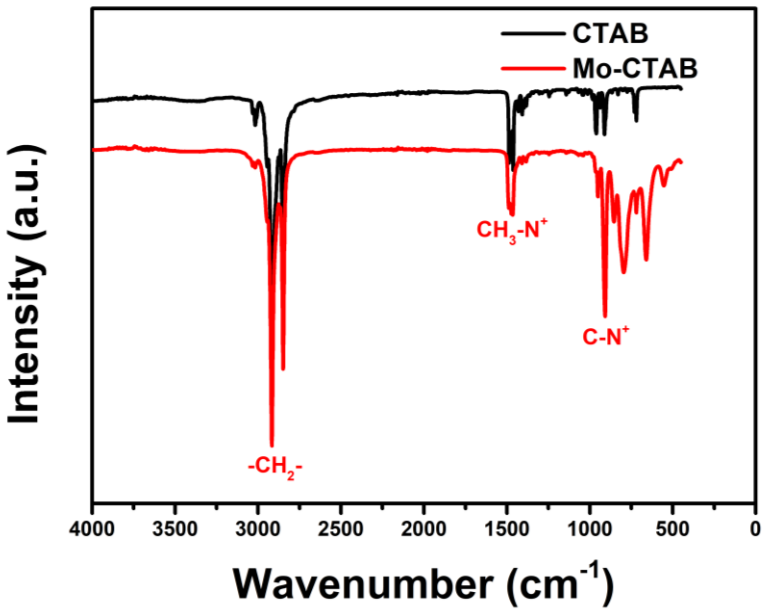

Fig. S11. FTIR spectra for CTAB and Mo-CTAB.

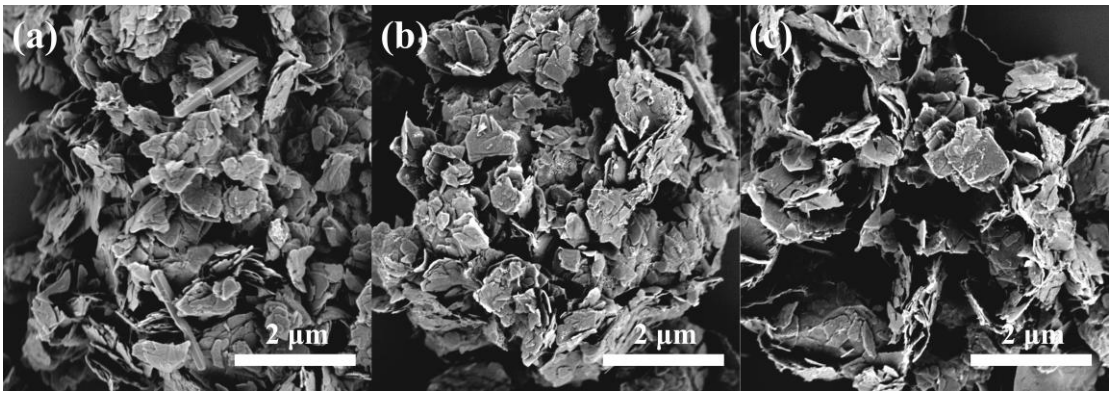

Fig. S12. SEM images for (a) Mo-MCM-0.1, (b) Mo-MCM-0.5 and (c) Mo-MCM-5 after calcination at 750 ºC.

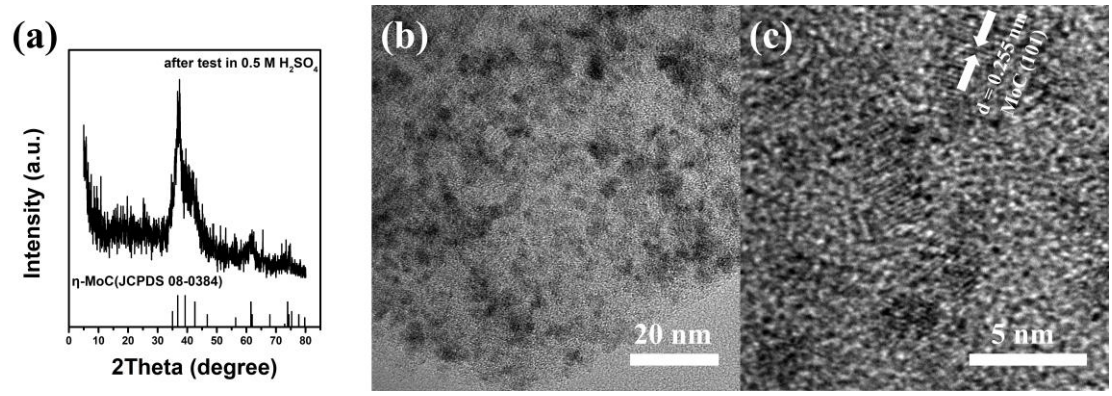

Fig. S13. XRD pattern (a) and TEM images (b, c) for nano-MoC/C-Ns-0.5 after long-term stability test in 0.5 M H_2SO_4.

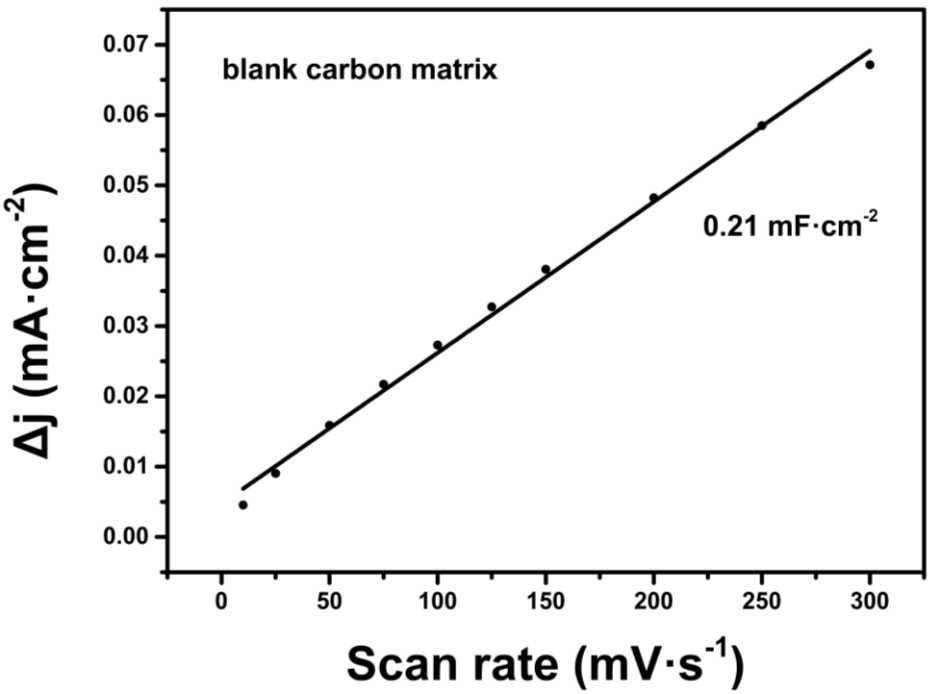

Fig. S14. Capacitive current at 150 mV as a function of scan rates for carbon matrix sample in 0.5 M H_2SO_4.

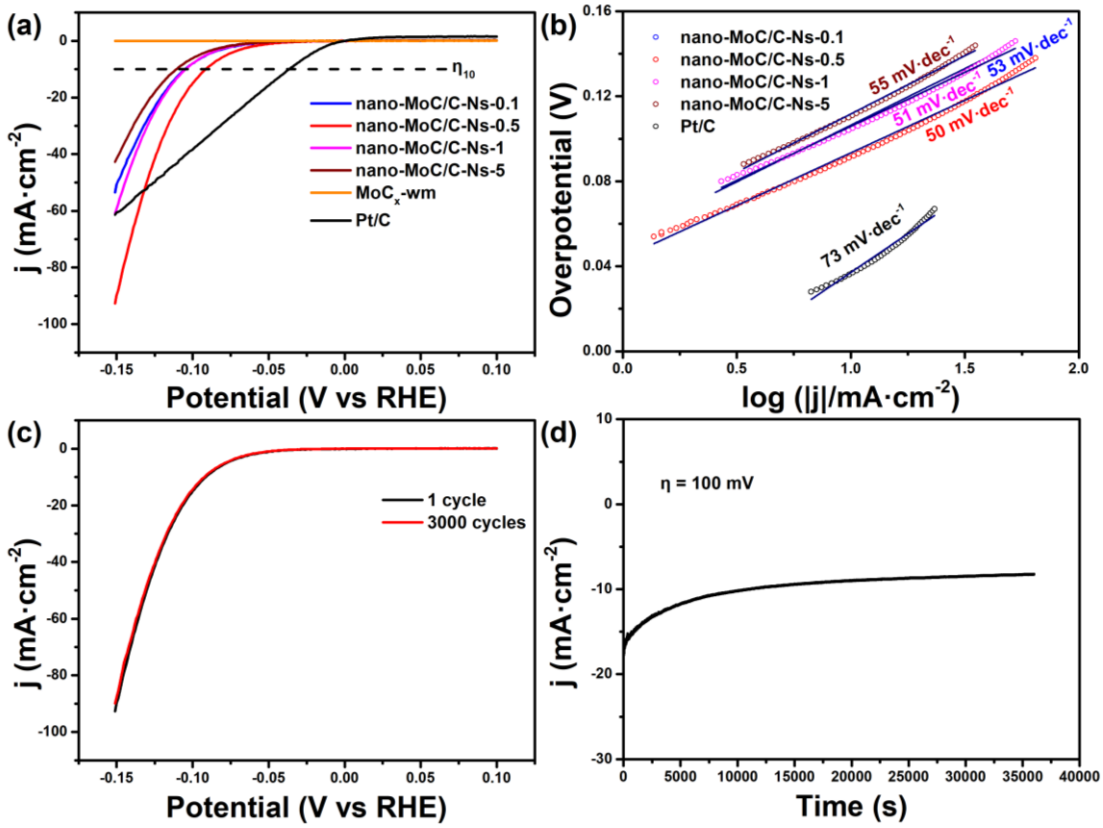

Fig. S15. (a) Polarization curves for nano-MoC/C-Ns-x samples, MoC_x-wm contrast sample and Pt/C. (b) Corresponding Tafel plots. (c) Initial polarization curve and curve after 3000 cycles for nano-MoC/C-Ns-0.5. (d) Time-dependent current density curve for nano-MoC/C-Ns-0.5 at η = 100 mV for 10 hours in 1 M KOH.

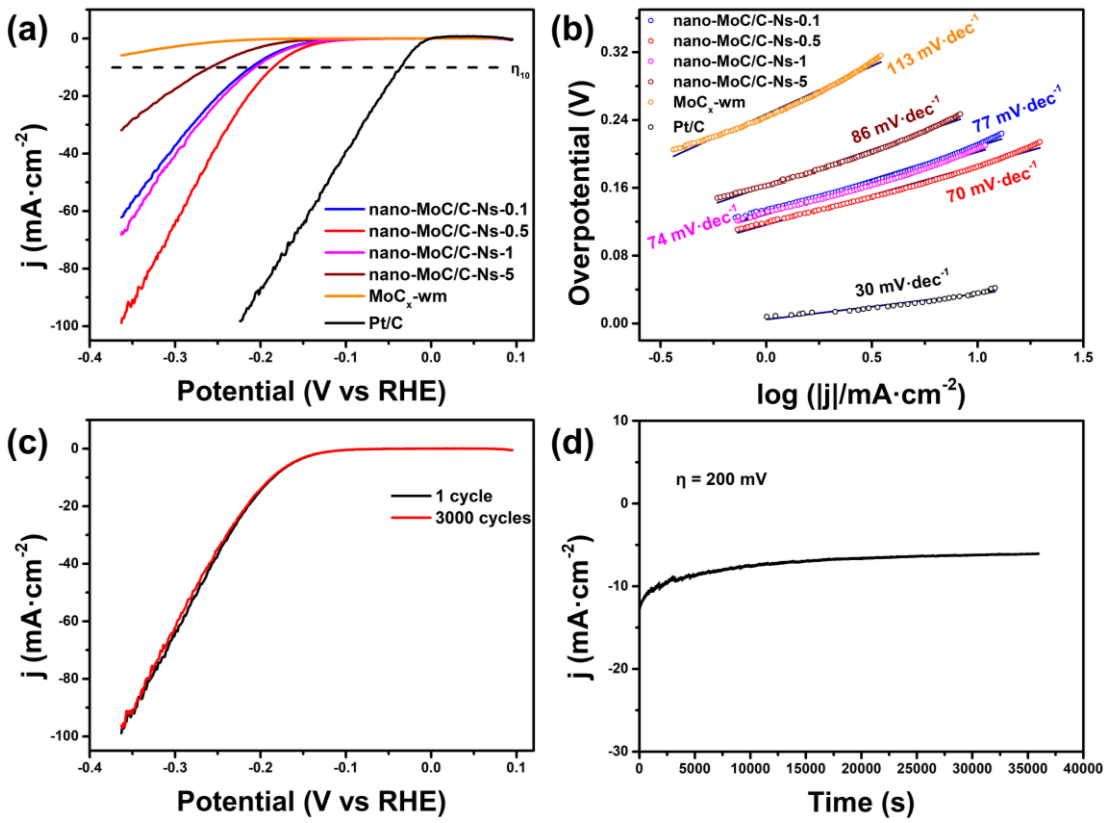

Fig. S16. (a) Polarization curves for nano-MoC/C-Ns-x samples, MoC_x-wm contrast sample and Pt/C. (b) Corresponding Tafel plots. (c) Initial polarization curve and curve after 3000 cycles for nano-MoC/C-Ns-0.5. (d) Time-dependent current density curve for nano-MoC/C-Ns-0.5 at η = 200 mV for 10 hours in 1 M PB.

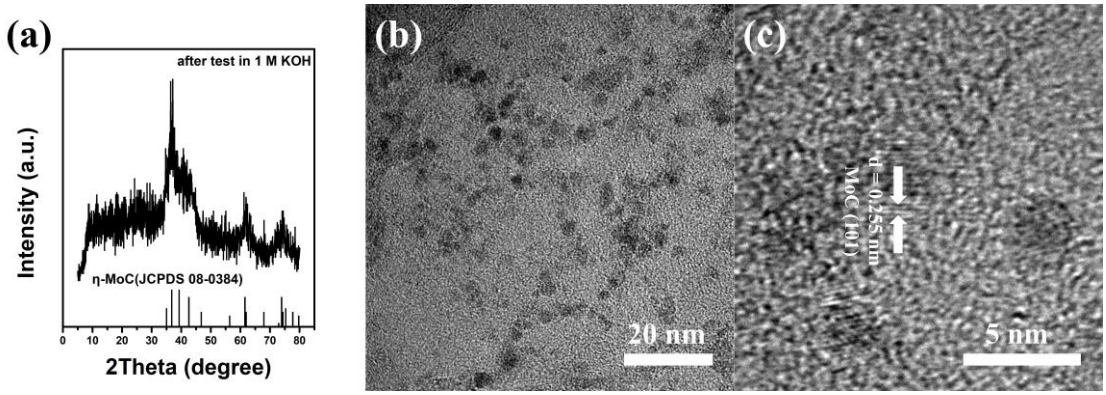

Fig. S17. XRD pattern (a) and TEM images (b, c) for nano-MoC/C-Ns-0.5 after long-term stability test in 1 M KOH.

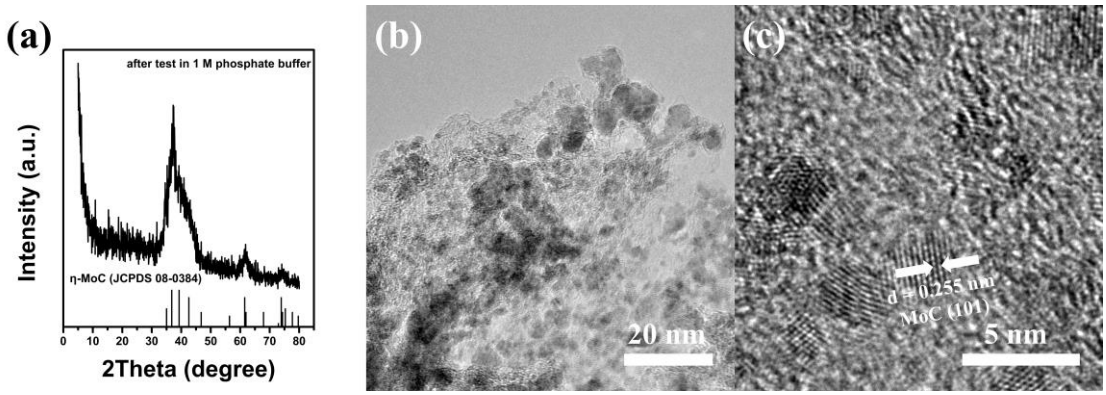

Fig. S18. XRD pattern (a) and TEM images (b, c) for nano-MoC/C-Ns-0.5 after long-term stability test in 1 M PB.

Table S1. The content of MoC in each nano-MoC/C-Ns-x samples.

Sample	MoC (wt. %)[a]	MoC (wt. %)[b]
nano-MoC/C-Ns-0.1	63.3	60.2
nano-MoC/C-Ns-0.5	67.8	66.6
nano-MoC/C-Ns-1	66.7	64.0
nano-MoC/C-Ns-5	67.1	64.7

a. Calculated by the TGA curves.

b. Quantified by ICP-AES. 5 mg of each nano-MoC/C-Ns-x sample is dispersed in 30 wt. % hydrogen peroxide solution and decomposed by stirring. The solution is then diluted to 50 ml after filtration for the ICP-AES test.

Table S2. XPS fitting results (peak position, peak area and species content) for nano-MoC/C-Ns-x samples.

Sample	species	B. E. (eV)		Area		Mo(II)/ Mo(III)	Mo(II) and Mo(III) (%)
		$3d_{5/2}$	$3d_{3/2}$	$3d_{5/2}$	$3d_{3/2}$		
nano-MoC/C-Ns-0.1	Mo(II)	228.3	231.2	2254	1502	0.19	54.6
	Mo(III)	228.8	231.8	9382	6255		
	Mo(IV)	229.7	233.2	5433	3622		
	Mo(VI)	232.5	235.3	4228	2818		
nano-MoC/C-Ns-0.5	Mo(II)	—	—	—	—	<0.01	49.1
	Mo(III)	228.7	231.8	8932	5955		
	Mo(IV)	229.7	233.1	5226	3484		
	Mo(VI)	232.5	235.4	4037	2692		
nano-MoC/C-Ns-1	Mo(II)	—	—	—	—	<0.01	39.8
	Mo(III)	228.8	231.7	8911	5940		
	Mo(IV)	229.6	233.2	5631	3754		
	Mo(VI)	232.3	235.4	7825	5216		
nano-MoC/C-Ns-5	Mo(II)	—	—	—	—	<0.01	26.7
	Mo(III)	228.8	232.1	5084	3390		
	Mo(IV)	229.5	233.2	5474	3650		
	Mo(VI)	232.4	236.0	8507	5671		

Table S3. Summary of nano-MoC/C-Ns-x, MoC_x-wm and Pt/C properties in HER process in 0.5 M H_2SO_4.

Sample	η_{10} (mV)	j_{200} ($mA \cdot cm^{-2}$)	Tafel slope ($mV \cdot dec^{-1}$)	j_0 ($mA \cdot cm^{-2}$)	C_{dl} ($mF \cdot cm^{-2}$)	ECSA (cm_{ECSA}^2)	R_{ct} (Ω)
nano-MoC /C-Ns-0.1	163	34	71	6.2×10^{-2}	44	78	77
nano-MoC /C-Ns-0.5	126	100	69	1.9×10^{-1}	60	106	25
nano-MoC /C-Ns-1	163	32	75	7.6×10^{-2}	30	53	67
nano-MoC /C-Ns-5	188	13	84	6.1×10^{-2}	21	38	99
MoC_x-wm	—	7	95	6.6×10^{-2}	11	19	214
Pt/C	28	—	32	6.0×10^{-1}	—	—	—

Table S4. Comparison of HER performance in acid media for nano-MoC/C-Ns with other electrocatalysts.

Catalyst	Loading ($mg \cdot cm^{-2}$)	Electrolyte	η (mV)	j ($mg \cdot cm^{-2}$)	Tafel slope ($mV \cdot dec^{-1}$)	Ref.
nano-MoC /C-Ns	1.13	0.5 M H_2SO_4	126	10	69	**This work**
MoC- graphene sheets	0.8	0.5 M H_2SO_4	221	10	88	[S2]
MoC/C	0.57	0.5 M H_2SO_4	144	20	63.6	[S3]
W-MoO_2 /MoC@PC	0.86	0.5 M H_2SO_4	209	20	96	[S4]
Mo_2C@NC	0.28	0.5 M H_2SO_4	124	10	60	[S5]
MoC@NCS	0.4	0.5 M H_2SO_4	81	10	43	[S6]
MoC-MoP/BCNC	1.09	0.5 M H_2SO_4	158	10	58	[S7]
N-Mo_xC@C	0.36	0.5 M H_2SO_4	172	10	60	[S8]
B-MoC	0.35	0.5 M H_2SO_4	285	10	128	[S9]
N, P-Mo_xC nanofibers	0.27	0.5 M H_2SO_4	107	10	65	[S10]
MoO_2/MoC@C	0.57	0.5 M H_2SO_4	133	20	77.3	[S11]
MoC_x@SWNTs	0.32	1 M $HClO_4$	345	10	115	[S12]
MoC/NPC @CNTs	0.34	0.5 M H_2SO_4	175	10	62	[S13]
nanoporous *η*-MoC NS	0.3	0.5 M H_2SO_4	122	10	53	[S14]
Mo_2C-0.5% Fe@NCF	1.6	0.5 M H_2SO_4	104	10	110	[S15]
β-Mo_2C-NC	0.19	0.5 M H_2SO_4	152	10	58	[S16]
MoC-Mo_2C	0.14	0.5 M H_2SO_4	126	10	43	[S17]
Mo_2C/NCF	0.28	0.5 M H_2SO_4	144	10	55	[S18]
CoP@NC	0.31	0.5 M H_2SO_4	78	10	49	[S19]
Mo_2N-Mo_2C	0.34	0.5 M H_2SO_4	157	10	55	[S20]
1T/2H-MoSSe	0.88	0.5 M H_2SO_4	161	10	52	[S21]

Table S5. TOF values for nano-MoC/C-Ns-x samples in all conditions at an overpotential of 150 mV.

Sample	TOF value (s^{-1})		
	Acid	Neutral	Alkaline
nano-MoC/C-Ns-0.1	4.9×10^{-3}	1.5×10^{-3}	4.1×10^{-2}
nano-MoC/C-Ns-0.5	2.0×10^{-2}	2.4×10^{-3}	6.8×10^{-2}
nano-MoC/C-Ns-1	4.8×10^{-3}	1.6×10^{-3}	4.6×10^{-2}
nano-MoC/C-Ns-5	2.1×10^{-3}	4.9×10^{-4}	3.2×10^{-2}

Table S6. The ECSA provided by each unit mass of Mo element.

Sample	ECSA (cm_{ECSA}^2)	Mo content (mg)[a]	ECSA/Mo ($cm^2\cdot mg^{-1}$)
nano-MoC/C-Ns-0.1	78	0.045	1733
nano-MoC/C-Ns-0.5	106	0.048	2208
nano-MoC/C-Ns-1	53	0.047	1128
nano-MoC/C-Ns-5	38	0.048	792

a. Calculated by TGA curves; the content here means the weight of Mo element on the working electrode.

Table S7. Summary of nano-MoC/C-Ns-x and Pt/C properties in HER process in 1 M KOH. MoC_x-wm is omitted here because the excessively low activity mixed with the instrument noise is difficult to tell apart.

Sample	η_{10} (mV)	Tafel slope ($mV \cdot dec^{-1}$)	j_0 ($mA \cdot cm^{-2}$)
nano-MoC/C-Ns-0.1	105	53	1.0×10^{-1}
nano-MoC/C-Ns-0.5	92	50	1.3×10^{-1}
nano-MoC/C-Ns-1	105	51	8.3×10^{-2}
nano-MoC/C-Ns-5	111	55	9.1×10^{-2}
Pt/C	37	73	3.2×10^{-1}

Table S8. Summary of nano-MoC/C-Ns-x, MoC_x-wm and Pt/C properties in HER process in 1 M PB.

Sample	η_{10} (mV)	Tafel slope ($mV \cdot dec^{-1}$)	j_0 ($mA \cdot cm^{-2}$)
nano-MoC/C-Ns-0.1	211	77	2.0×10^{-2}
nano-MoC/C-Ns-0.5	185	70	2.2×10-2
nano-MoC/C-Ns-1	207	74	1.8×10^{-2}
nano-MoC/C-Ns-5	259	86	1.3×10^{-2}
MoC_x-wm	—	113	6.6×10^{-3}
Pt/C	36	30	7.0×10^{-1}

Table S9. Comparison of HER performance in alkaline media for nano-MoC/C-Ns with other electrocatalysts.

Catalyst	Loading ($mg \cdot cm^{-2}$)	Electrolyte	η (mV)	j ($mg \cdot cm^{-2}$)	Tafel slope ($mV \cdot dec^{-1}$)	Ref.
nano-MoC /C-Ns	1.13	1 M KOH	92	10	50	**This work**
W-MoO2 /MoC@PC	0.86	1 M KOH	208	20	81	[S4]
Mo_2C@NC	0.28	1 M KOH	60	10	—	[S5]
MoC@NCS	0.4	1 M KOH	89	10	51	[S6]
MoC-MoP/BCNC	1.09	1 M KOH	137	10	64	[S7]
MoC-HAs	0.41	1 M KOH	128	10	82	[S22]
B-MoC	0.35	1 M KOH	349	10	85	[S9]
N, P-Mo_xC nanofibers	0.27	1 M KOH	135	10	57	[S10]
MoO_2/MoC@C	0.57	1 M KOH	203	20	105	[S11]
nanoporous η-MoC NS	0.3	1 M KOH	119	10	39	[S14]
Mo_2C-0.5% Fe@NCF	1.6	1 M KOH	65	10	76	[S15]
β-Mo_2C-NC	0.19	1 M KOH	135	10	52	[S16]
Co, Mo_2C-CNF	1	1 M KOH	128	10	60	[S23]
MoC-Mo_2C	0.14	1 M KOH	120	10	42	[S17]
Mo_2C/NCF	0.28	1 M KOH	100	10	65	[S18]
Cu NDs/Ni_3S_2 NTs-CFs	0.52	1 M KOH	128	10	76	[S24]
CoP@NC	0.31	1 M KOH	129	10	58	[S19]
Ni/Mo_2C-PC	0.5	1 M KOH	179	10	101	[S25]
Mo_2N-Mo_2C	0.34	1 M KOH	154	10	68	[S20]
Ni NP/Ni-N-C	0.24	1 M KOH	147	10	114	[S26]
Co-BDC/MoS_2	0.16	1 M KOH	248	10	86	[S27]

Table S10. Comparison of HER performance in neutral media for nano-MoC/C-Ns with other electrocatalysts.

Catalyst	Loading ($mg \cdot cm^{-2}$)	Electrolyte	η (mV)	j ($mg \cdot cm^{-2}$)	Tafel slope ($mV \cdot dec^{-1}$)	Ref.
nano-MoC /C-Ns	1.13	1 M PB	185	10	70	**This work**
Mo_2C@NC	0.28	0.1 M PB	156	10	—	[S5]
B-MoC	0.35	0.1 M PBS	722	10	263	[S9]
Co, Mo_2C-CNF	1	1 M PBS	206	10	93	[S23]
Mo_2C−GNR	0.28	1 M PBS	266	10	74	[S28]
Co-Mo_2C@NC	—	0.2 M PBS	260	10	118	[S29]
Mo_2C@N-CNF	0.255	0.1 M PBS	437	10	77	[S30]
Mo_2C/MoP @NPC	—	1 M PBS	228	10	125	[S31]
P-W_2C@NC	3.5	0.1 M PB	185	10	—	[S32]
Mo-N/C@N-C	0.84	1 M PB	240	10	＞100	[S33]
Mo_2C/MoO_2	0.29	0.1 M PBS	290	10	—	[S34]

Reference:

S1. J. Wang, W. Wang, L. Ji, S. Czioska, L. Guo and Z. Chen, *ACS Appl. Energy Mater.*, 2018, **1**, 736–743.

S2. C. He and J. Tao, *RSC Adv.*, 2016, **6**, 9240–9246.

S3. C. Lv, Z. Huang, Q. Yang, G. Wei, Z. Chen, M. G. Humphrey and C. Zhang, *J. Mater. Chem. A*, 2017, **5**, 22805–22812.

S4. C. Lv, Z. Huang, Q. Yang and C. Zhang, *Energy Technol.*, 2018, **6**, 1707–1714.

S5. Y. Liu, G. Yu, G.-D. Li, Y. Sun, T. Asefa, W. Chen and X. Zou, *Angew. Chemie Int. Ed.*, 2015, **54**, 10752–10757.

S6. J.-T. Ren, L. Chen, C.-C. Weng, G.-G. Yuan and Z.-Y. Yuan, *ACS Appl. Mater. Interfaces*, 2018, **10**, 33276–33286.

S7. N. Chen, Q. Mo, L. He, X. Huang, L. Yang, J. Zeng and Q. Gao, *Electrochim. Acta*, 2019, **299**, 708–716.

S8. T. Xiong, J. Jia, Z. Wei, L. Zeng, Y. Deng, W. Zhou and S. Chen, *Chem. Eng. J.*, 2019, **358**, 362–368.

S9. Q. Lin, C. Shang, Z. Chen, X. Wang and G. Zhou, *Int. J. Hydrogen Energy*, 2020, **45**, 30659–30665.

S10. L. Ji, J. Wang, X. Teng, H. Dong, X. He and Z. Chen, *ACS Appl. Mater. Interfaces*, 2018, **10**, 14632–14640.

S11. C. Lv, Z. Huang, Q. Yang and C. Zhang, *Inorg. Chem. Front.*, 2018, **5**, 446–453.

S12. T. Cui, J. Dong, X. Pan, T. Yu, Q. Fu and X. Bao, *J. Energy Chem.*, 2019, **123**, 123–127.

S13. X. Ji, K. Wang, Y. Zhang, H. Sun, Y. Zhang, T. Ma, Z. Ma, P. Hu and Y. Qiu, *Sustain. Energy Fuels*, 2020, **4**, 407–416.

S14. C. Tang, H. Zhang, K. Xu, Q. Zhang, J. Liu, C. He, L. Fan and T. Asefa, *J. Mater. Chem. A*, 2019, **7**, 18030–18038.

S15. J. Huang, J. Wang, R. Xie, Z. Tian, G. Chai, Y. Zhang, F. Lai, G. He, C. Liu, T. Liu, P. R. Shearing and D. J. L. Brett, *J. Mater. Chem. A*, 2020, **8**, 19879–19886.

S16. J. Wang, S. Li, J. Hu, S. Niu, Y. Li and P. Xu, *Inorg. Chem. Front.*, 2020, **7**, 3620–3626.

S17. H. Lin, Z. Shi, S. He, X. Yu, S. Wang, Q. Gao and Y. Tang, *Chem. Sci.*, 2016, **7**, 3399–3405.

S18. Y. Huang, Q. Gong, X. Song, K. Feng, K. Nie, F. Zhao, Y. Wang, M. Zeng, J. Zhong and Y. Li, *ACS Nano*, 2016, **10**, 11337–11343.

S19. F. Yang, Y. Chen, G. Cheng, S. Chen and W. Luo, *ACS Catal.*, 2017, **7**, 3824–3831.

S20. H. Yan, Y. Xie, Y. Jiao, A. Wu, C. Tian, X. Zhang, L. Wang and H. Fu, *Adv. Mater.*, 2018, **30**, 1704156.

S21. Z. Lin, B. Lin, Z. Wang, S. Chen, C. Wang, M. Dong, Q. Gao, Q. Shao, T. Ding, H. Liu, S. Wu and Z. Guo, *ChemCatChem*, 2019, **11**, 2217–2222.

S22. H. Wang, X. Xu, B. Ni, H. Li, W. Bian and X. Wang, *Nanoscale*, 2017, **9**, 15895–15900.

S23. J. Wang, R. Zhu, J. Cheng, Y. Song, M. Mao, F. Chen and Y. Cheng, *Chem. Eng.*

J., 2020, **397**, 125481.

S24. J.-X. Feng, J.-Q. Wu, Y.-X. Tong and G.-R. Li, *J. Am. Chem. Soc.*, 2018, **140**, 610–617.

S25. Z.-Y. Yu, Y. Duan, M.-R. Gao, C.-C. Lang, Y.-R. Zheng and S.-H. Yu, *Chem. Sci.*, 2017, **8**, 968–973.

S26. C. Lei, Y. Wang, Y. Hou, P. Liu, J. Yang, T. Zhang, X. Zhuang, M. Chen, B. Yang, L. Lei, C. Yuan, M. Qiu and X. Feng, *Energy Environ. Sci.*, 2019, **12**, 149–156.

S27. D. Zhu, J. Liu, Y. Zhao, Y. Zheng and S.-Z. Qiao, *Small*, 2019, **15**, 1805511.

S28. W. Gao, Y. Shi, Y. Zhang, L. Zuo, H. Lu, Y. Huang, W. Fan and T. Liu, *ACS Sustain. Chem. Eng.*, 2016, **4**, 6313–6321.

S29. M. Wang, S. Dipazir, P. Lu, Y. Wang, M. Yuan, S. Li and G. Zhang, *J. Colloid Interface Sci.*, 2018, **532**, 774–781.

S30. Z.-Y. Wu, B.-C. Hu, P. Wu, H.-W. Liang, Z.-L. Yu, Y. Lin, Y.-R. Zheng, Z. Li and S.-H. Yu, *NPG Asia Mater.*, 2016, **8**, e288–e288.

S31. J.-Q. Chi, W.-K. Gao, J.-H. Lin, B. Dong, K.-L. Yan, J.-F. Qin, Z.-Z. Liu, Y.-M. Chai and C.-G. Liu, *J. Colloid Interface Sci.*, 2018, **513**, 151–160.

S32. G. Yan, C. Wu, H. Tan, X. Feng, L. Yan, H. Zang and Y. Li, *J. Mater. Chem. A*, 2017, **5**, 765–772.

S33. R. Cheng, H. He, Z. Pu, I. S. Amiinu, L. Chen, Z. Wang, G. Li and S. Mu, *Electrochim. Acta*, 2019, **298**, 799–805.

S34. M. Liu, Y. Yang, X. Luan, X. Dai, X. Zhang, J. Yong, H. Qiao, H. Zhao, W. Song and X. Huang, *ACS Sustain. Chem. Eng.*, 2018, **6**, 14356–14364.